

REGIONAL ANAESTHESIA

Virtual reality-based simulator for training in regional anaesthesia

O. Grottke^{1 2*}, A. Ntoubas³, S. Ullrich⁴, W. Liao⁵, E. Fried⁴, A. Prescher⁶, T. M. Deserno⁵,
T. Kuhlen⁴ and R. Rossaint¹

¹Department of Anaesthesiology and ²Institute for Laboratory Animal Science, RWTH Aachen University Hospital, Germany. ³Department of Anaesthesiology and Intensive Care, University of Amiens, Picardie, France. ⁴Virtual Reality Group, ⁵Department of Medical Informatics and ⁶Institute for Anatomy, RWTH Aachen University Hospital, Aachen, Germany

*Corresponding author. E-mail: ogrottke@ukaachen.de

Background. The safe performance of regional anaesthesia (RA) requires theoretical knowledge and good manual skills. Virtual reality (VR)-based simulators may offer trainees a safe environment to learn and practice different techniques. However, currently available VR simulators do not consider individual anatomy, which limits their use for realistic training. We have developed a VR-based simulator that can be used for individual anatomy and for different anatomical regions.

Methods. Individual data were obtained from magnetic resonance imaging (MRI) and magnetic resonance angiography (MRA) without contrast agent to represent morphology and the vascular system, respectively. For data handling, registration, and segmentation, an application based on the Medical Imaging Interaction Toolkit was developed. Suitable segmentation algorithms such as the fuzzy c-means clustering approach were integrated, and a hierarchical tree data structure was created to model the flexible anatomical structures of peripheral nerve cords. The simulator was implemented in the VR toolkit ViSTA using modules for collision detection, virtual humanoids, interaction, and visualization. A novel algorithm for electric impulse transmission is the core of the simulation.

Results. In a feasibility study, MRI morphology and MRA were acquired from five subjects for the inguinal region. From these sources, three-dimensional anatomical data sets were created and nerves modelled. The resolution obtained from both MRI and MRA was sufficient for realistic simulations. Our high-fidelity simulator application allows trainees to perform virtual peripheral nerve blocks based on these data sets and models.

Conclusions. Subject-specific training of RA is supported in a virtual environment. We have adapted segmentation algorithms and developed a VR-based simulator for the inguinal region for use in training for different peripheral nerve blocks. In contrast to available VR-based simulators, our simulation offers anatomical variety.

Br J Anaesth 2009; **103**: 594–600

Keywords: anaesthetic techniques, regional; anaesthetic techniques, regional, inguinal; education; model, computer simulation

Accepted for publication: May 14, 2009

Regional anaesthesia (RA) has been used increasingly during the past four decades¹ due to the perceived advantages of reduced postoperative pain, earlier mobility, shorter hospital stay, and lower costs.² However, RA requires good theoretical, practical, and non-cognitive skills to allow trainees to achieve confidence in performing RA and to keep complications to a minimum.³ Current

training methods for RA include cadavers, video teaching, ultrasound guidance, and simple virtual patient modelling.⁴ The advantage of using simulators in medicine is the creation of a realistic environment with standardized and reproducible scenarios without endangering patients.⁵ The first anaesthesia simulator, SIM1, was described in 1969,⁶ and the progress in computer technology led to the

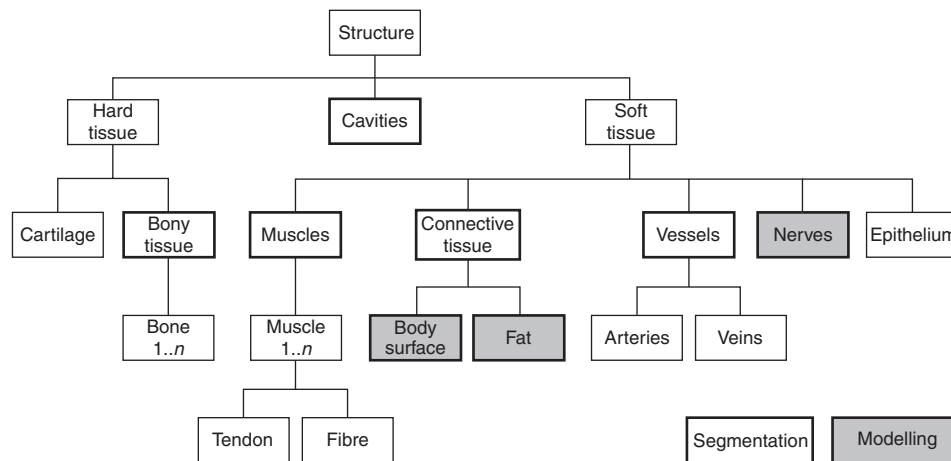


Fig 1 Ontology of tissue intended to be used by the simulator. Bold-lined boxes and shaded boxes indicate direct segmentation and modelling, respectively.

development of different systems including high-fidelity simulators.⁷ However, the limited numbers of virtual reality (VR)-based simulators for RA narrow their use for training purposes. Technically, VR simulators do not consider individual patients' anatomy and cannot be adapted to different regions such as the inguinal region, spine, neck, or arm. Therefore, we have started to develop a VR-based simulator on the basis of different patients' anatomies to allow trainees to practise their technical skills on a variety of virtual patients. We present the data extraction, design, and implementation of a localized patient model for RA of the inguinal region. Novel simulation algorithms are described and discussed in comparison with related work.

Methods

Catalogue of requirements

According to the Haptics Optional Surgical Training System (HOSTS), which is developed for the US Army,⁸ a training system has to fulfil several criteria. These include:

- to identify the right injection site and proper injection angle;
- to keep the hand position at the proper angle and stable during the injection, which requires knowledge of the appropriate hand position for each block position and proper needle placement during injection;
- to ensure that a nerve is not pierced; and
- to feature the ability to assess nerve stimulation.

A realistic model for RA should provide a virtual environment that can be adapted easily to the individual patient's anatomy and also to different procedures on different body regions. The incorporation of haptic feedback requires the discrimination of different types of tissue and thus necessitates the modelling of certain structures.

Therefore, a hierarchical ontology has been created by systematic classification in accordance with anatomical properties (Fig. 1). Bony tissue, muscles, connective (adipose) tissue, and vessels must be imaged, whereas skin, fat, and nerves can be simulated from these data.

Data acquisition

For the purpose of non-invasive data acquisition, the use of computed tomography imaging and the routinely deployed injection of contrast agents were excluded. Instead, data from magnetic resonance imaging (MRI) with a field strength of 1.5 T were used (Philips Achieva 1.5T A series, The Netherlands). To extract the vascular system, a time of flight (TOF) magnetic resonance angiography (MRA) sequence was applied (512×512 pixels, 100 slices, resolution 0.88 mm×0.88 mm×3.0 mm, repetition time: 23.0 ms, echo time: 6.9 ms, flip angle: 23°). Bone, musculature, and soft tissues were captured using a T1-weighted fast-field-echo (FFE) sequence (480×480 pixel, 100 slices, resolution 0.94 mm×0.94 mm×3.0 mm, repetition time: 302.6 ms, echo time: 4.6 ms, flip angle: 80°). In both MRA and MRI, a four-channel SENSE body coil was applied to increase the signal-to-noise ratio (SNR) and to shorten the scan times.

Image processing

Using the Medical Imaging Interaction Toolkit (MITK),⁹ the Insight Segmentation and Registration Toolkit (ITK),¹⁰ and the Visualization Toolkit (VTK),¹¹ an application was developed to assist data handling, registration, and segmentation. Affine registration of MRI and MRA was performed automatically applying the ITK modules for mutual information and evolutionary computing for metric and optimization, respectively. Mutual information measures the information that two random variables (here the two images during their iterative alignment) share. An evolutionary algorithm is a generic population-based

optimization procedure that uses mechanisms inspired by biological evolution: reproduction, mutation, recombination, and selection.

On the basis of a manually positioned seed point, the fuzzy c-means clustering algorithm,¹² which allows one piece of data to belong to two or more clusters, was applied for automatic segmentation of the muscular structure. A geometric deformable model approach was used for bones.¹³ For the vascular system, a region growing algorithm was applied. Mathematical morphology operators are applied to smooth the soft tissue labels and, in particular, the surface of the body. As a result, each voxel was labelled as either of the tissue classes (skin, fat, vessel, muscle, and bone) or background.

Nerve modelling and simulation

Nerves cannot be sufficiently visualized with MRI or MRA. Therefore, a hierarchical data structure was created to simulate nerve cords (Fig. 2). Functional nodes and spline curves represent nerve sections. Each spline curve is defined by control points, in the neighbourhood of the segmented vessels, which can be placed in the virtual environment using anatomical landmarks such as branches of vessel trees.

In addition to the vessel morphology, the modelled nerve nodes are attached to movable anatomical structures, for example, bones and muscles. Each node holds a list of splines, while each spline in turn features two control points. These control points are shared between neighbouring splines to create continuous curves and branches. Nerves which innervate muscles (other types of nerves are irrelevant for our purpose) end at the adjacent muscle with a myoeceptor. This anatomical entity translates the electric impulse into muscle stimuli. In our data structure, these nerve ends are represented by specialized control points. By abstraction, both geometric and functional characteristics can be reused for other anatomical cords such as blood vessels or lymph vessels.

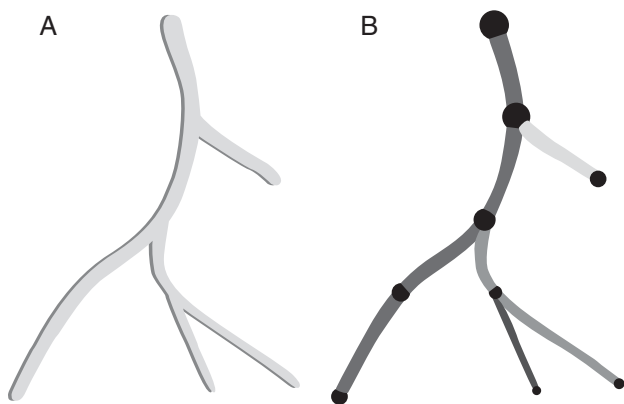


Fig 2 A virtual nerve tree (A) is composed of piece-wise splines (shaded differently) between the control points and branches with shared control points (B).

Simulator application

The application was implemented in the virtual toolkit ViSTA and applies several modules for collision detection, virtual humanoids, interaction, and visualization.¹⁴ We developed a system architecture to separate data structures from algorithms, which in turn contributed to the extensibility and interchangeability of data sets for patient-specific data.¹⁵ For the electric impulse transmission, a novel approach based on electric distance was developed. It was used to determine which nerve cords are reached and to calculate the intensity of the electric impulse. Visualization algorithms were developed to allow explorative analysis and interactive rendering of geometric representations of the virtual patient and the instruments. A geometry algorithm called vertex blending was used to create a deformable skin surface for changing the posture of the patient, for palpation, and for muscle response.¹⁶ Two approaches were established to visualize virtual nerve cords. Polygonal lines were used to incorporate thin nerve cords. To adequately represent thicker cords, so-called tubelets were applied, which are accelerated and shaded by modern graphics cards.¹⁷ The visualization of muscle twitches (caused by electric nerve stimulation and propagated through fat tissue to the skin surface) is based on morphing algorithms. Two geometries including the anatomical region of interest were applied, one with the relaxed muscle and another with the contracted one. According to the triggering of nerves and the calculated contraction state of the muscles, we morphed the meshes in between these two extremes to produce reasonable intermediary results.

Interaction algorithms have been created to support a range of different input devices [e.g. VR-devices like tracking systems and a six-degree-of-freedom mouse, and also keyboard and a two-dimensional (2D) mouse]. These were used to navigate through the virtual environment and to change the view relative to the virtual patient. A picking metaphor (similar to drag and drop on 2D desktops) allowed to interactively manipulate the posture of the virtual patient and thus provided better access for the insertion of the needle. Support for customized haptic input devices was implemented and used for palpation¹⁸ to localize the needle injection site realistically and for needle operations. All input data can optionally be recorded during training for evaluation afterwards.

Results

Data acquisition

The inguinal region of five individuals was recorded using the MRI/MRA imaging protocol (Table 1). The group of subjects, males and females, included a range in weight [mean (SD) 73 (20) kg], size [mean (SD) 173 (10) cm], and age [mean (SD) 26 (9) yr].

Table 1 Biometric data of five subjects who have been scanned with MRI and MRA protocols to create models of the inguinal region

Gender	Weight (kg)	Size (cm)	Age (yr)
Female	55	155	26
Female	61	162	18
Male	61	172	26
Male	79	179	41
Male	110	187	20

Segmentation

The MRI allows the segmentation procedures to differentiate between fat, muscle, and bone (Fig. 3). Vessels are also visible. The high-contrasted body-to-background contour is used for registration. The segmentation processes requires only simple user interactions and then continue automatically. As it can be seen (Fig. 3), the user is guided step by step through the registration, segmentation, and labelling process. Only a few manual interactions are necessary since the application supports storage and reload of configuration files. The total processing time is ~ 25 min on a standard desktop PC.

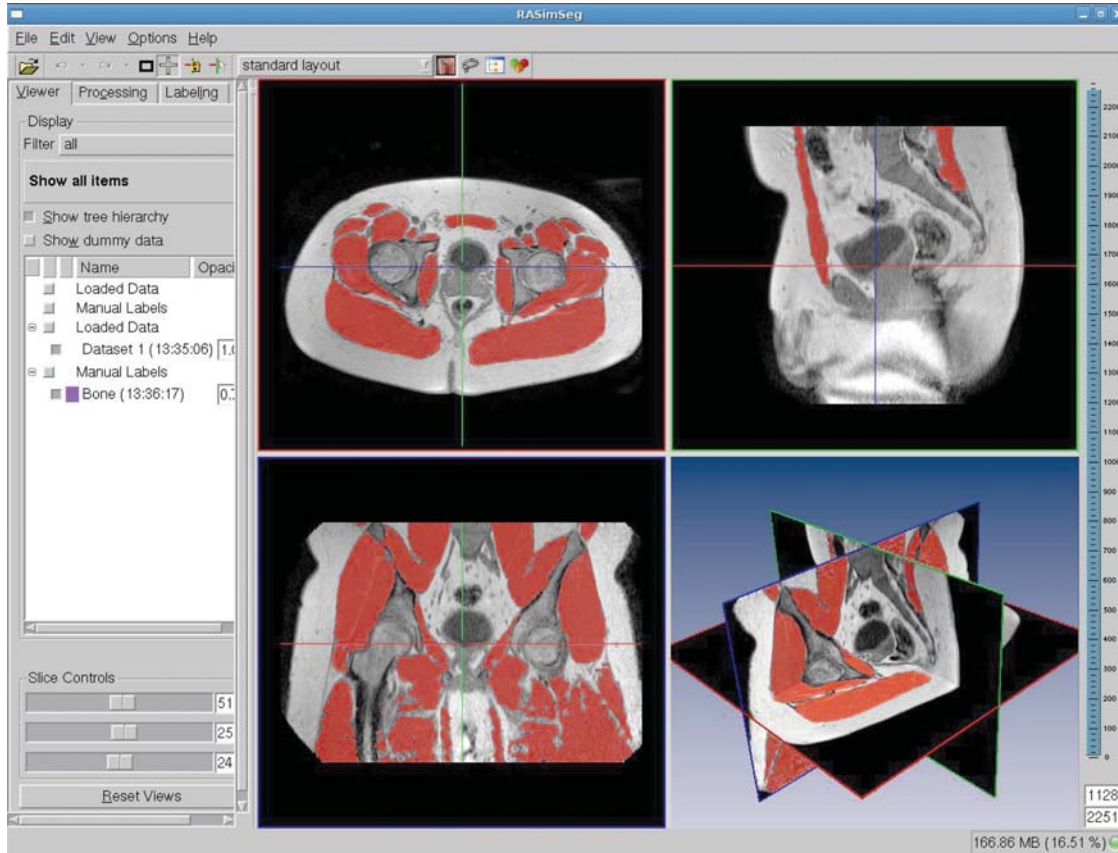
Nerve modelling and simulation

The result of nerve modelling for Subject 3 shows that the spline approximation yields smooth transitions. On the

basis of the ViSTA toolkit, the data sets can be visualized on a standard PC monitor (Fig. 4A) and also in large immersive virtual environments (Fig. 4B). Irrespective of the visualization environment, they can be manipulated interactively.

Simulator application

The algorithm for the electric distance approach for impulse transmission determines the shortest path of electrons through inhomogeneous tissues (Fig. 5). At first, a special search data structure based on path-finding algorithms is created. This data structure is also referred to as a roadmap.¹⁹ To construct such a data structure, sample points are randomly distributed within the area around the needle. Accepted samples (i.e. inside the virtual body) either cover a volume around themselves (called guards) or are used to connect guard nodes with each other (called connectors). The desired percentage of coverage, the radius of the sphere of a guard (the extent of the volume it represents), and the maximum distance between guards and connectors are parameters that define the quality of the simulation, and also influence the processing time. From these samples, a bi-directional graph can be generated²⁰ whose edge weights are closely related to the electric resistance of the tissue between the nodes.

**Fig 3** MITK-based application for segmentation with coronal, transversal, and sagittal views from MRI scans.

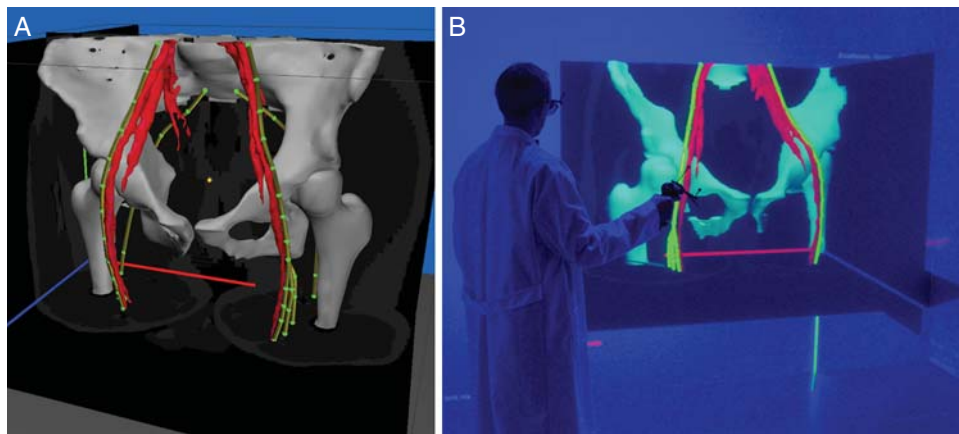


Fig 4 Inguinal region with combined 3D data sets (A, shown on a desktop monitor) from segmentation (bones and blood vessels) and modelling (nerve cords). These data sets can also be visualized and manipulated in large immersive virtual environments (B, I-Space from Barco GmbH, Germany).

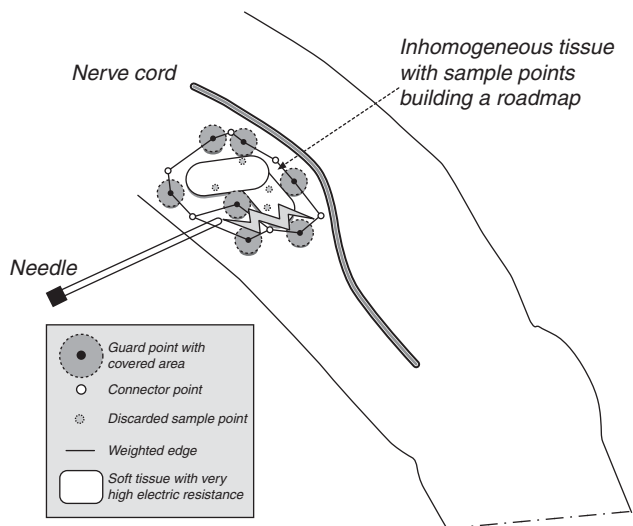


Fig 5 Schematic overview of electric impulse transmission. The special data structure (roadmap) contains electric resistance values assigned to weighted edges between sample points. The electrons travel on the path with lowest electric resistance. In this example, they do not cross the high resistance soft tissue.

The construction of this roadmap cannot be performed in real time and thus had to be pre-calculated. In a second step, the built data structure was used to determine the shortest path in terms of electric resistance from the tip of the needle to the nerve whose control points are part of the samples. This step is performed iteratively in each simulation cycle during the search process with the needle.

The PHANTOM Omni[®] Haptic Device (SensAble Technologies, USA) was used to control the instruments and to provide force feedback (Fig. 6). As a first approach, the simulator computes a very rudimentary haptic feedback once the virtual needle has entered the body. This is based on the virtual proxy approach²¹ and the use of constant material properties for fat tissue and muscle tissue. The stimulation properties of the virtual needle (e.g. impulse strength and impulse duration) can be changed via



Fig 6 VR-based setup of the RA simulator application. The trainee controls the virtual needle through a PHANTOM Omni Haptic device.

a 2D graphical user interface in order to support a systematic search process for the nerve.

Discussion

The development of new simulators and the recognition of their utility for training and continuing medical education have led to widespread use in medicine.²² However, the use of manikins to train RA is limited by inter-patient variability, inaccurate representation of biological tissue, and physical wear from repeated use. Sophisticated interactive VR are a potentially valuable way to overcome these constraints, encompassing the advantages of a flexible environment with the allowance of dynamic view changes and accurate training of sterical relationships. Although not all VR simulators are suitable for all training purposes,²³ the majority of studies assessing VR-based training tools have shown a beneficial effect.^{24–26}

The development of appropriate anatomical VR models necessitates detailed visualization of relevant structures. One of the first approaches was the Visible Human data

set²⁷ that has been manually labelled in the VOXEL-MAN project.²⁸ Networks have also contributed greatly to the creation of new data sets and visualization for anatomical teaching and surgical simulation.²⁹⁻³⁰ It is important to distinguish between anatomical visualization, surgical planning, and surgical simulation. All rely on anatomical data sets, but the dynamics of simulation requires deformable geometry and data optimization for real-time interaction. This means that visualization algorithms must share CPU processing time with physics-based simulation to deform and move geometry, for example, in one time-step, the simulation must be updated and the scene redrawn. If these time steps take too long, the frame rate gets too low, resulting in jerky animations. Although current available VR-based RA simulators do allow practice of manual skills in different body regions, they are limited by their lack of variance and realism.³¹⁻³² Data sets, such as labelled volumes and 3D triangular mesh geometries representing organs provided by the Visible Human Project³³ and Zygote Media Group, Inc.,³⁴ form the basis of these simulators. These commercially available data sets contain one set of high-quality 3D geometry models for each gender. The provision of only one anatomical data set does not allow anatomical variation, which is an important feature to allow decision-making under varying conditions. Another example is the interactive anatomical models of Primal Pictures, Ltd.,³⁵ which are very detailed and feature biomechanical animations for the musculoskeletal system. However, these data sets are only available as rendered 2D images and movie clips. Therefore, these data cannot be used for simulation. In contrast, our flexible and dynamic concept of simulation allows the exchange of patient-specific data sets, implementation of sophisticated haptics, and the extension to new regions for other procedures.

Since direct exposure of nerve trees with T1-weighted MRI does not provide sufficient SNR to support automatic segmentation, angiographic and morphologic MR scans were performed consecutively to realize the simulations. The choice of sequence for MRA was not difficult, since the widely used TOF sequence³⁶⁻³⁷ also produced good results in our approach. However, it was more challenging to find an adequate sequence for MRI morphology. T2-weighted turbo spin-echo (T2 TSE), T1-weighted magnetization-prepared rapid acquired gradient echo (T1 MP-RAGE), T1-weighted chemical shifting, and T1 FFE were probed, and T1 FFE was chosen. For data acquisition, we used Siemens TrioTrim with 1.5 T and Philips Achieva with 1.5 and 3 T. The best image quality for both angiography and morphology was achieved using a 1.5 T. For our purposes, image quality was not enhanced with increased magnetic field. A recent report described non-contrast-enhanced MRA using a 7 T MRI.³⁸ The increased spatial resolution of up to 200 μm offered by 7 T MRI³⁹ may be useful for RA simulation data, when it becomes available.

It is preferable that the segmentation process is initialized automatically with minimal user interaction. In our approach, only two seed points had to be specified; one for each vascular tree in the region, although the clustering algorithm is automatically initialized with a predefined number of three classes to separate the T1-weighted data into background, soft tissue, and the remaining tissue. Further automatization of the process can be achieved using active shape models for the vessel trees. Such statistical models of the shape of objects can be iteratively deformed to fit the object in a new image.⁴⁰ An advantage of the chosen MITK platform is that algorithms for image processing and segmentation can easily be added and integrated.

Virtual nerve cords are represented by rigid geometry in the French simulator SAILOR³¹ and simulator being developed by Hu and colleagues.³² In our approach, nerves are constructed with piece-wise spline curves. This allows unrestricted modelling and furthermore enables fast deformation. Most importantly, control points can be transformed locally within standard deviations and thus new anatomical configurations can be created in order to provide challenges in training.

For the simulator application, the electric impulse transmission is one of the most essential parts and requires a proper and accurate simulation. Our approach for electric impulse transmission based on electric distance allows for higher accuracy than a geometric-based heuristic method.³² The usual trade off compromising real time for higher accuracy is circumvented by pre-calculation of the roadmap and optimization techniques for the search in the data structure during run-time of the algorithm. The visualization of nerve cords with virtual tubelets originates from an approach developed to display particle trajectories in computational fluid dynamics.¹⁷ A fast rendering speed and a convincing 3D effect are the advantages over standard polygonal tubes for visualization.

The simulator supports a wide range of output devices for representation and input devices which allows use in different environments. Depending on needs and economic considerations, the simulator can be run on a low cost PC and also in larger environments which allow intuitive 3D exploration with realistic interaction. Since it has been shown that VR training without haptic feedback is not realistic, our simulator integrates a PHANTOM Omni[®] Haptic Device for 3D movements,⁴¹ in comparison with other simulators which use a 2D mouse for interaction and do not have input devices for intuitive steering of the needle or haptical force feedback.³¹ Future work will include the development of other regions of interest and an evaluation comparing traditional methods of learning against VR-based training. It is intended also to incorporate a sophisticated haptic simulation for realistic tool-tissue interaction to enhance user acceptance. Therefore, tissue properties will be acquired and used in a novel physics-based soft-tissue simulation.

In summary, we developed a flexible training environment with VR by using multimodal representations of both visual and rudimentary haptics with intuitive interactions and a plausible simulation. This VR-based simulator is the first of its kind, which was created using a number of different patients to form a flexible and dynamic learning environment to train, and improve, their skills in different peripheral nerve blocks.

Funding

This work was supported by a grant from the German Research Foundation (DFG, KU 1132/4-1, LE 1108/8-1, RO 2000/7-1).

References

- Bartussek E, Fatehi S, Motsch J, Grau T. Survey on practice of regional anaesthesia in Germany, Austria, and Switzerland. Part I: Quality assurance and training concepts. *Anaesthesist* 2004; **53**: 836–46
- Evans H, Steele SM, Nielsen KC, Tucker MS, Klein SM. Peripheral nerve blocks and continuous catheter techniques. *Anesthesiol Clin North Am* 2005; **23**: 141–62
- Smith AF, Pope C, Goodwin D, Mort M. What defines expertise in regional anaesthesia? An observational analysis of practice. *Br J Anaesth* 2006; **97**: 401–7
- Bröking K, Waurick R. How to teach regional anaesthesia. *Curr Opin Anaesthesiol* 2006; **19**: 526–30
- Wong AK. Full scale computer simulators in anaesthesia training and evaluation. *Can J Anaesth* 2004; **51**: 455–64
- Denson JS, Abrahamson S. A computer-controlled patient simulator. *J Am Med Assoc* 1969; **208**: 504–8
- Cumin D, Merry AF. Simulators for use in anaesthesia. *Anaesthesia* 2007; **62**: 151–62
- Available from <http://www.energjd.com> (accessed March 20, 2009)
- Available from <http://www.mitk.org> (accessed March 20, 2009)
- Available from <http://www.itk.org> (accessed March 20, 2009)
- Available from <http://vtk.org> (accessed March 20, 2009)
- Bezdek JC. *Pattern Recognition with Fuzzy Objective Function Algorithms*. New York: Plenum Press, 1981
- Caselles V, Catte F, Coll T, Dibos F. A geometric model for active contours. *Numer Math* 1993; **66**: 1–31
- Assenmacher I, Kuhlen T. The ViSTA virtual reality toolkit. *Proceedings of the IEEE VR SEARIS*. 2008
- Ullrich S, Valvoda JT, Prescher A, Kuhlen T. Comprehensive Architecture for simulation of the human body based on functional anatomy. *Proc BVM* 2007; 328–32
- Lewis JP, Corder M, Fong N. Pose space deformation: a unified approach to shape interpolation and skeleton-driven deformation. *Proc Comput Graph Interact Tech* 2000; 165–72
- Schirski M, Kuhlen T, Hopp M, Adomeit P, Pischinger S, Bischof C. Virtual tubelets—efficiently visualizing large amounts of particle trajectories. *Comput Graph* 2005; **29**: 17–27
- Ullrich S, Mendoza J, Ntoubas A, Rossaint R, Kuhlen T. Haptic pulse simulation for virtual palpation. *Proc BVM* 2008; 187–91
- Simeon T, Laumond JP, Nissoux C. Visibility-based probabilistic roadmaps for motion planning. *Adv Robot J* 1999; **6**: 14
- Salomon B, Gerber M, Lin MC, Manocha D. Interactive navigation in complex environments using path planning. *Proceedings of Symposium on Interactive 3D Graphics*. 2003; 41–50
- Ruspini D, Khatib O. Dynamic models for haptic rendering systems. *ARK*. 1998; 523–32
- Scalese RJ, Obeso VT, Issenberg SB. Simulation technology for skills training and competency assessment in medical education. *J Gen Intern Med* 2008; **23**: 46–9
- Friedl R, Preisack MB, Klas W, et al. Virtual reality and 3D visualizations in heart surgery education. *Heart Surg Forum* 2002; **5**: E17–21
- Gurusamy K, Aggarwal R, Palanivelu L, Davidson BR. Systematic review of randomized controlled trials on the effectiveness of virtual reality training for laparoscopic surgery. *Br J Surg* 2008; **95**: 1088–97
- Lim MW, Burt G, Rutter SV. Use of three-dimensional animation for regional anaesthesia teaching: application to interscalene brachial plexus blockade. *Br J Anaesth* 2005; **94**: 372–7
- Letterie GS. Medical education as a science: the quality of evidence for computer-assisted instruction. *Am J Obstet Gynecol* 2003; **188**: 849–53
- Available from http://www.nlm.nih.gov/pubs/factsheets/visible_human.html/ (accessed March 20, 2009)
- Available from <http://www.voxel-man.de/> (accessed March 20, 2009)
- Available from <http://www.medicalvisualisation.co.uk> (accessed March 20, 2009)
- Available from <http://3dah.miralab.unige.ch/> (accessed March 20, 2009)
- Bibin L, Lecuyer A, Burkhardt JM, Delbos A, Bonnet M. SAILOR: a 3-D medical simulator of loco-regional anaesthesia based on desktop virtual reality and pseudo-haptic feedback. *Proc ACM Int Symp VRST* 2008; 97–100
- Hu J, Lim Y, Tardella N, Chang C, Warren L. Localized virtual patient model for regional anaesthesia simulation training system. *Medicine Meets Virtual Reality* 2007; 185–90
- Ackerman MJ. The visible human project. *Proc IEEE* **86**: 504–11
- Available from <http://www.zygote.com> (accessed March 20, 2009)
- Available from <http://www.primalpictures.com> (accessed March 20, 2009)
- Hiai Y, Kakeda S, Sato T, et al. 3D TOF MRA of intracranial aneurysms at 1.5 T and 3 T: influence of matrix, parallel imaging, and acquisition time on image quality—a vascular phantom study. *Acad Radiol* 2008; **15**: 635–40
- Du YP, Jin Z. Simultaneous acquisition of MR angiography and venography (MRV). *Magn Reson Med* 2008; **59**: 954–8
- Maderwald S, Ladd SC, Gizewski ER, et al. To TOF or not to TOF: strategies for non-contrast-enhanced intracranial MRA at 7 T. *MAGMA* 2008; **21**: 159–67
- Cho ZH, Kim Y, Han J, et al. New brain atlas—mapping the human brain in vivo with 7.0 T MRI and comparison with post-mortem histology: will these images change modern medicine? *Int J Imaging Syst Technol* 2008; **18**: 2–8
- Cootes TF, Taylor CJ, Cooper DH, Graham J. Active shape models—their training and application. *Comput Vis Image Underst* 1995; **61**: 38–59
- Madan AK, Frantzides CT, Tebbit C, Quiros RM. Participants' opinions of laparoscopic training devices after a basic laparoscopic training course. *Am J Surg* 2005; **189**: 758–61